Dalton Transactions

ROYAL SOCIETY OF CHEMISTRY

PERSPECTIVE

View Article Online
View Journal | View Issue

Cite this: *Dalton Trans.*, 2025, **54**, 15686

Present state of knowledge on the electronic structure and oxidation state of iron in the brown ring complex: a long-standing debatable issue in undergraduate chemistry courses†

Udita Das,[a] Asim K. Das,[b] Ankita Das*[c] and Dhrubajyoti Mondal*[d]

Received 4th June 2025,
Accepted 23rd August 2025

DOI: 10.1039/d5dt01316j

rsc.li/dalton

In terms of electronic structure, the century-old, well-known brown ring complex formed in the classical brown ring test employed in the qualitative analysis of nitrate (and nitrite) is still a matter of debate among both theoretical and experimental chemists. The extensive π-bonding in the Fe–N–O linkage complicates the prediction of the real oxidation state of iron in the brown ring complex, involving the non-innocent NO ligand that can have different chemical states to tune the oxidation state of iron in the complex. This article summarises the present-day knowledge of the possible electronic structures of the quartet $\{Fe(NO)\}^7$ moiety (S = 3/2) of the brown ring complex. Experimental observations (isomer shift of ^{57}Fe in MB spectrum, EPR and IR data, X-ray crystal structure data, *etc.*) along with the consideration of the basic required conditions to accommodate the large number of remaining σ-donor neutral ligands ($5H_2O$) support the most probable oxidation state of iron as an intermediate state of +2 and +3, but closer to +3.

Introduction

In the classical "brown-ring" test for nitrate in aqueous solution in undergraduate analytical chemistry, the addition of a small amount of freshly prepared $FeSO_4$ or Mohr's salt solution to an aqueous solution of nitrate, followed by the careful addition of a small amount of concentrated sulphuric acid along the sides of the test tube containing the aqueous solution of Fe(II) and NO_3^- produces a brown iron nitrosyl complex, called the brown ring complex, denoted by $[Fe(H_2O)_5(NO)]^{2+}$, at the liquid–liquid interface.[1–3] The involved reactions and the appearance of the brown ring complex at the liquid–liquid interface are shown in Fig. 1.

The brown ring complex is unstable in terms of NO loss in aqueous solution. It may be noted that nitrite (NO_2^-) also responds to this test.[4] In fact, thermodynamically, both nitrate and nitrite are almost equally powerful oxidising agents, and nitrite can oxidise Fe(II) to Fe(III) in the same way to generate NO.[5] Besides this, under acidic conditions, nitrous acid produced from nitrite readily undergoes disproportionation to produce NO and NO_3^- (eqn (1)):[5]

$$3HNO_2 \rightleftharpoons NO_3^- + 2NO + H_2O + H^+ \quad (1)$$

Possible electronic structures of the brown ring complex: the non-innocent nature of the NO ligand

The odd-electron molecule NO, a 15e species with the unpaired electron in the π-ABMO (antibonding molecular orbital, π*-MO), is a well-known non-innocent ligand[6–10] that may exist in the complex as neutral NO, cationic NO^+ (isoelectronic with the well-known π-acid ligands CO and CN^-) and anionic NO^- (isoelectronic with the dioxygen ligand O_2)[11–36] which means that the brown ring complex likely has one of different possible electronic structures,[11,12] as shown in Table 1. In terms of the geometry of the M–N–O linkage, it can have the two modes:[11–14] the bent mode, characterised by an M–N–O bond angle < 165°, and the linear mode, characterised by an M–N–O bond angle > 165°. There is actually a correlation between the N–O stretching frequency (ν_{NO}) and the Fe–N–O bond angle in non-heme $\{FeNO\}^7$ (Enemark–Feltham notation[15]) complexes, which was first established by Chavez and coworkers.[16] Non-heme $\{FeNO\}^7$ complexes are broadly categorized into two spin states:[11,12] ls-$\{FeNO\}^7$ (total spin, S = 1/2) and hs-$\{FeNO\}^7$ (total spin, S = 3/2). The spin state is primarily

[a]*Department of Chemistry, Indian Institute of Science Education and Research (IISER) Bhopal, Bhopal Bypass Road, Bhauri, 462066 Bhopal, Madhya Pradesh, India. E-mail: udita0505@gmail.com*
[b]*Department of Chemistry, Visva Bharati University, Santiniketan 731235, India. E-mail: asimkumar.das@visva-bharati.ac.in*
[c]*School of Chemical Sciences, Indian Association of Cultivation for the Science (IACS), Kolkata 32, India. E-mail: csad2329@iacs.res.in*
[d]*Department of Chemistry, Visva Bharati University, Santiniketan 731235, India. E-mail: dhrubajyoti.mondal@visva-bharati.ac.in*

†This article is dedicated to Late Prof. D. Banerjea, Sir Rashbehari Ghose Professor, Department of Chemistry, University of Calcutta, India.

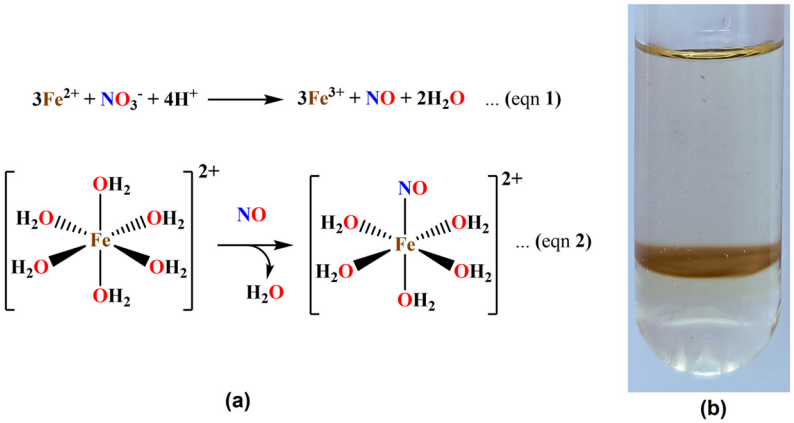

Fig. 1 (a) Involved reactions in the formation of the brown ring complex. (b) Appearance of the brown ring complex at the liquid–liquid interface.

Table 1 Possible electronic structures of the brown ring complex[11]

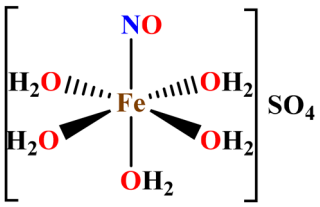

Fe^{II} + NO → hs-$\{FeNO\}^7$ (total spin, $S = 3/2$)

Electronic Structure	Iron spin state		NO spin state	Coupling
$Fe(I)–NO^+$	$Fe(I)$: d^7	($S = 3/2$)	NO^+ ($S = 0$)	—
$Fe(II)–NO^\bullet$	$Fe(II)$: d^6	($S = 2$)	$NO^\bullet$ ($S = 1/2$)	AF
		($S = 1$)		F
$Fe(III)–NO^-$	$Fe(III)$: d^5	($S = 5/2$)	NO^- ($S = 1$)	AF
		($S = 3/2$)	NO^- ($S = 0$)	—
		($S = 1/2$)	NO^- ($S = 1$)	F

governed by the ligand environment around the iron center.[11,12] Complexes bearing the strong-field ligands, such as macrocyclic N4-type frameworks or other ligands with high ligand-field strength, typically stabilize the low-spin configuration.[12] In contrast, complexes incorporating the weak-field ligands, most commonly polypyridine derivatives or other nitrogen-based heterocycles, favor the high-spin state.[12]

Enemark–Feltham notation of the electronic structure of the 'M(NO)' moiety in the nitrosyl complexes

According to the Enemark–Feltham notation,[15] the '$\{M(NO)_y\}$' moiety present in a complex is represented by $\{M(NO)_y\}^x$, where the superscript x denotes the total number of valence electrons (*i.e.*, the sum of the metal-d and the NO-π* electrons), and y denotes the number of NO groups in the 'M(NO)' moiety. For the electron count (x), we may consider one electron per NO ligand and an appropriate d^n configuration of the metal to maintain the overall charge of the complex (*i.e.*, $x = y + n$). Thus, for the purpose of electron counting (x), consideration of the actual oxidation states of the metal and NO ligand in the complex is not required. This is illustrated in the following representative six-coordinate mononitrosyl ($y = 1$) complexes:[15]

$[Cr(CN)_5(NO)]^{3-}$: $\{Cr^{II}(NO)\}^5$, *i.e.*, $d^4 + 1 = 5$, linear M–N–O linkage (176°)

$[V(CN)_5(NO)]^{3-}$: $\{V^{II}(NO)\}^4$, *i.e.*, $d^3 + 1 = 4$, linear M–N–O linkage (176°)

$[Mn(CN)_5(NO)]^{3-}$: $\{Mn^{II}(NO)\}^5$, *i.e.*, $d^5 + 1 = 6$, linear M–N–O linkage (174°)

$[Fe(CN)_5(NO)]^{2-}$: $\{Fe^{III}(NO)\}^6$, *i.e.*, $d^5 + 1 = 5$, linear M–N–O linkage (178°)

$[Co(NH_3)_5(NO)]^{2+}$: $\{Co^{II}(NO)\}^8$, *i.e.*, $d^7 + 1 = 8$, bent M–N–O linkage (119°)

It is evident that in the six-coordinate mononitrosyl complexes, for higher values of x (>6), to maintain the 18e rule, the bent M–N–O linkage is quite expected as in this mode, NO acts as a 1e donor ligand while for the smaller values of x (≤6), to maintain the 18e rule, the linear M–N–O linkage is quite reasonable as in this mode, NO acts as a 3e donor ligand. It has already been mentioned that Chavez and coworkers[16] have established a correlation between the N–O stretching frequency (ν_{NO}) and the Fe–N–O bond angle in non-heme $\{FeNO\}^7$ complexes. This correlation confirms the proposed Fe–N–O angle of ~160° in the brown ring compound.

Nitrosyl complexes

Linear M–N–O linkage[11,12]

When NO coordinates as NO^+, in terms of electron count, NO acts as a 3e donor ligand: donation of the unpaired electron present in the π-ABMO to reduce the metal (M) centre by 1e followed by the σ-donation of a lone pair present in the non-bonding MO or weakly σ-ABMO as the HOMO (highest occupied MO) of NO^+ produced by the 1e transfer from the HOMO of NO to the metal centre. Thus, the produced NO^+ acts as a weak 2e donor ligand in the Lewis sense, and at the same time, it can act as a potential π-acid ligand like CO, which is isoelectronic with NO^+ that receives back electrons from the

metal d-orbital through the π-backbonding, d (metal) → π*-MO (NO^+). This π-backbonding is favoured for the linear M–N–O linkage due to the better overlap between the metal d-orbital and π*-MO of NO^+, and this reduces the IR-stretching frequency (ν_{NO}, cm^{-1}) of NO^+. In fact, for the nitrosyl complexes having NO^+ as the ligand, ν_{NO} increases compared to that of free neutral NO (ν_{NO} = 1876 cm^{-1}) due to the loss of one electron from the π*-MO of NO, but it decreases compared to that of free NO^+ (ν_{NO} = 2387 cm^{-1} in $NOBF_4$)[37] because of the electron acceptance in the π*-MO of NO^+ through the π-backbonding, d (metal) → π*-MO (NO^+).[11–14] In fact, for the linear nitrosyl complexes (NO^+ as the ligand), ν_{NO} lies in the range 1660–1900 cm^{-1}, satisfying the condition: 2387 cm^{-1} (free NO^+) > ν_{NO} (in the complex) > 1876 cm^{-1} (free NO).[13,14] Here, it is assumed that the σ-donation of the lone pair present in the nonbonding MO or weakly σ*-MO does not affect much the ν_{NO} value.[13,14]

The N–O stretch (ν_{NO}) value in the linear M–N–O linkages depends on the degree of oxidation of NO in the nitrosyl complex. This is illustrated by two representative complexes. In sodium nitroprusside (SNP), $Na_2[Fe(CN)_5(NO)]$, the octahedral anionic moiety $[Fe(CN)_5(NO)]^{2-}$ with a linear FeNO unit shows a very high N–O stretch value (ν_{NO} = 1939 cm^{-1})[17,18] indicative of distinct NO oxidation. The N–O stretch value is found a little low (ν_{NO} = 1903 cm^{-1})[19,20] in the complex $[Ru(NH_3)_5(NO)]Cl_3$, indicative of partial NO oxidation.

Bent M–N–O linkage[11,12]

When NO coordinates as neutral NO, it acts as a 1e donor ligand. The unpaired electron of NO makes a covalent-like linkage with the metal's unpaired electron in a d-orbital, as in the organic nitroso compounds (R–N═O) housing a lone pair on the sp^2-N to make the linkage bent, as also predicted by the VSEPR (valence shell electron pair repulsion) theory. When the metal centre is electron rich or in a low oxidation state, it becomes readily oxidisable, and an electron can be transferred to the singly occupied π*-MO (or the singly occupied sp^2-N orbital in terms of valence bond theory, VBT) of NO to reduce it to NO^- (isoelectronic with O_2) which in turn can act as a strong 2e π-donor ligand but a weak π-acceptor ligand.[12] In this case, in terms of electron counting, NO effectively acts as a 1e donor ligand by considering the 1e reduction of NO to NO^- by the oxidisable metal centre. Both neutral NO and NO^- produce a bent M–N–O linkage. It may be noted that NO^- is isoelectronic with O_2, which also coordinates in a bent end-on fashion in many complexes, as in haemoglobin and myoglobin.[38–41] In the formation of NO^-, it receives an electron in π*-MO of NO and consequently, ν_{NO} (1358 cm^{-1} in NaNO)[42] decreases compared to free NO (= 1876 cm^{-1}). In general, we have the order: ν_{NO} (= 1660–1900 cm^{-1} in the linear mode of coordination) > ν_{NO} (= 1525–1680 cm^{-1} in the bent mode of coordination). Here, it is important to mention that for the $\{FeNO\}^7$ systems, the N–O stretching band (both IR and Raman active) usually appears in the range of ~1700–1800 cm^{-1} and the Fe–N–O angle is correlated with the N–O stretch, where a higher N–O stretching frequency is correlated with a more linear Fe–N–O unit.[11,12,16,43] Strong anionic coligands (see Table 2) reduce the iron's effective nuclear charge, decreasing the π-donation from the singly occupied π* orbitals of $^3NO^-$ to the electron-rich iron center.[12] This weakens both the Fe–NO and N–O bonds (because of the increased electron density in the antibonding π* orbitals of NO), lowering their stretching frequencies (ν_{NO} drops down to the 1700 cm^{-1} region).[12] Conversely, in the presence of neutral coligands (*e.g.*, TPA, BMPA, TMPza, and H_2O), the metal center becomes less electron-rich, which enhances π-donation from the $^3NO^-$ ligand. This increased π-interaction strengthens the Fe–NO bond, makes the Fe–NO unit more linear, and shifts the N–O stretching frequency closer to ~1800 cm^{-1} (see Table 2).[12] Not only the electronic factor, but the steric factor can also play an important role in controlling the Fe–N–O bond angle.[44]

Iron–nitrosyl complexes

Heme and non-heme iron–nitrosyl complexes are considered as the important intermediates in biological processes.[11,12,23,26] Examples of low-spin (ls) heme iron–nitrosyl complexes and high-spin (hs) non-heme iron–nitrosyl complexes are known.[12,23] In fact, Fe(II) non-heme iron–nitrosyls have been studied as the models for the corresponding O_2 complexes to understand the mechanistic pathways of activity of non-heme iron enzymes.[27–30] The Lehnert group[26] prepared a complete series of high spin hs-$\{Fe–NO\}^{6–8}$ complexes ($[Fe(TMG_3tren)(NO)]^{2+}$) using the TMG_3tren coligand (Fig. 2). These complexes, generated *via* redox transformations of the hs-$\{FeNO\}^7$ species to hs-$\{FeNO\}^6$ (by one-electron oxidation) and hs-$\{FeNO\}^8$ (by one-electron reduction), have been extensively investigated through the different experimental techniques, such as X-ray crystallography, MCD, XANES/EXAFS, Mössbauer spectroscopy, and theoretical DFT studies. These studies have established the fact that these redox transformations are all metal-centered and the corresponding complexes represent hs-Fe(II)–$^3NO^-$ (hs-$\{FeNO\}^8$, S = 1, ν_{NO} = 1618 cm^{-1}), Fe(III)–$^3NO^-$ (hs-$\{FeNO\}^7$, S = 3/2, ν_{NO} = 1739 cm^{-1}) and ^{3}Fe(IV)–$^3NO^-$ (hs-$\{FeNO\}^6$, S = 1, ν_{NO} = 1879 cm^{-1}) systems.

In contrast, for the corresponding low-spin (ls) iron–nitrosyl complexes (*i.e.* ls-$\{FeNO\}^{6–8}$) having the cyclam-acetate coligand, prepared by Wieghardt's group,[31] such redox transformations are found to be NO-centered (Fig. 3), *i.e.*, ls-Fe(II)–$^1NO^-$ (ls-$\{FeNO\}^8$, S = 0, ν_{NO} = 1271 cm^{-1}), ls-Fe(II)–$NO^\bullet$ (ls-$\{FeNO\}^7$, $S = \frac{1}{2}$, ν_{NO} = 1607 cm^{-1}) and ls-Fe(II)–NO^+ (ls-$\{FeNO\}^6$, S = 0, ν_{NO} = 1903 cm^{-1}).

In the hs-$\{FeNO\}^{6–8}$ complexes, the NO^- ligand acts predominantly as a strong π-donor ligand, and the degree of covalency in the Fe–NO bond increases with the increasing positive oxidation state of iron. It is reflected in the increasing trend of Fe–NO bond strength in the order: hs-$\{FeNO\}^6$ ($\nu_{Fe–NO}$ = 594 cm^{-1}) > hs-$\{FeNO\}^7$ ($\nu_{Fe–NO}$ = 484 cm^{-1}) > hs-$\{FeNO\}^8$ ($\nu_{Fe–NO}$ = 435 cm^{-1}). It may be noted[12,23] that the ls-$\{FeNO\}^7$ complexes (S = 1/2) can be reversibly reduced to the corresponding stable ls-$\{FeNO\}^8$ complexes (S = 0, diamagnetic); the reduction is ligand (NO) centered and it occurs at extremely negative redox potentials. In contrast, hs-$\{FeNO\}^7$ non-heme complexes (S = 3/2) experience the metal-centered reduction,

Table 2 Comparison of structural and spectroscopic parameters for 6-coordinate hs-{FeNO}^{7} complexes

Complexes	ν_{NO} (cm^{-1})	Fe–N distance (Å)	Fe–N–O angle (°)	N–O distance (Å)	Mössbauer [δ (mm s^{-1}) and $\lvert\Delta E_Q\rvert$ (mm s^{-1})]	Total spin (g values)	Geometry	Ref.
[Fe(BMPA)(OTf)$_2$(NO)]	1848	1.76	180	1.12	—	S = 3/2 (g = 4, 2)	Octahedral	45
[Fe(H$_2$O)$_5$(NO)][Ga(fpin)$_2$(H$_2$O)]$_2$·8.34H$_2$O	1843	1.79	161	1.14	0.66, 2.03	S = 3/2	Octahedral	46
[Fe(H$_2$O)$_5$(NO)][Fe(fpin)$_2$(H$_2$O)]$_2$·8.31H$_2$O	1841	1.78	162	1.13	0.66, 2.03	S = 3/2	Octahedral	46
[Fe(T1Et$_4$^{i}PrIP)(THF)(OTf)(NO)]$^+$	1831	1.76	169–174	1.15	—	S = 3/2 (g = 3.90, 2.01)	Octahedral	16
[(L$_{KP}$)Fe(NO)(H$_2$O)]$^{2+}$	1826	1.75	173	1.16	—	S = 3/2 (g = 3.893, 2.002)	Octahedral	47
[Fe(N3Py^{2Ph}SEtCN)(NO)](BF$_4$)$_2$	1812	—	165 (DFT)	—	0.67, 2.20	S = 3/2 (g = 4.07, 3.91, and 1.99)	Octahedral	48
[Fe(TPA)(CH$_3$CN)(NO)](ClO$_4$)$_2$	1810	—	—	—	—	S = 3/2 (g = 3.90, 2.02)	Octahedral	49
[Fe(H$_2$O)$_5$(NO)]$^{2+}$	1810	—	—	—	0.76, 2.1	S = 3/2 (g = 4.04, 4.04, 2.0)	Octahedral	50
[Fe(TPA)(OTf)(NO)](OTf)	1806	1.76	170	1.14		S = 3/2 [g = 3.91, 2.0 (in dcm)]	Octahedral	51
[Fe(6Me$_3$TPA)(BF)(NO)](ClO$_4$)	1802	—	—	—	—	S = 3/2 (g = 4.02, 3.93, 1.95)	Octahedral	52
[Fe(TMPzA)Cl(NO)]BPh$_4$	1796	1.74	157	1.15	—	—	Octahedral	53
[Fe(TPA)(BF)(NO)]ClO$_4$	1794	1.72–1.74	155/162	1.14–1.15	—	S = 3/2 (g = 4.05, 3.87, 1.99)	Octahedral	52
[Fe(T1Et$_4$iPrIP)(NO)(H$_2$O)$_2$]$^{2+}$	1791	1.77–1.79	162–165	1.12–1.13	—	S = 3/2 (g = 4 and 2)	Octahedral	43
{Fe(BMPA-Pr)(NO)}$_6$(OTf)$_6$	1784	1.76	149	1.17	—	Perturbed S = 3/2	Octahedral	49
{Fe(BMPA-Pr)(NO)}$_6$(ClO$_4$)$_6$	1777	1.72	152	1.18	—	Perturbed S = 3/2	Octahedral	49
[Fe(6-COO$^-$-tpa)(NO)]$^+$	1752	1.75	166	1.11	—	S = 3/2 (g = 3.66, 2.03)	Octahedral	54
[Fe(BMPA-tBu$_2$PhO)(NO)(OTf)]	1742	1.78	163	1.10	—	S = 3/2 (g = 3.91, 2.0)	Octahedral	51
cis-[(Cyclam)Fe(NO)I]I	1726	—	—	—	0.64, 1.78	S = 3/2 (g = 3.99, 1.98)	Octahedral	55
[Fe(BMPA-Pr)(Cl)(NO)]	1726	1.78	152	1.15	—	S = 3/2 (g = 3.95, 2.0)	Octahedral	49
[Fe(Me$_3$TACN)(N$_3$)$_2$(NO)]	1690	1.74	156	1.14	0.62, 1.28	S = 3/2 (g = 4, 2)	Octahedral	56
[Fe(S^{Me2}N$_4$(tren)(NO))]$^+$	1685	1.77	152	1.12	—	S = 3/2 (g = 4.41, 3.60, 1.98)	Octahedral	57
[Fe(NO)(Me$_3$TACN)((OSiPh$_2$)$_2$O)]	1680	1.74 (DFT)	144 (DFT)	1.20 (DFT)	0.52, 0.80	S = 3/2 (g = 4.08, 3.93, 1.99)	Octahedral	55 and 58
Fe(NO)(Me$_3$TACN)(S$_2$SiMe$_2$)	1659 (DFT)	1.71 (DFT)	149 (DFT)	1.19 (DFT)	0.50, 1.08	S = 3/2 (g = 4.06, 3.86, 2.00)	Octahedral	59
deflavo-FDP(NO)$_2$	1749 (aq)	—	—	—	0.74, 1.85	—	—	60

TPA = tris(2-pyridylmethy1)amine; fpin = perfluoropinacolato-κ^2O,O'; 6Me$_3$TPA = tris((6-methyl-2-pyridyl)methyl)amine; BF = benzoylformate; Me$_3$TACN = *N*,*N*′,*N*″-trimethyl-1,4,7-triazacyclononane; dcm = dichloromethane, BMPA-tBu$_2$PhOH = *N*-(3,5-di-*tert*-butyl-2-hydroxybenzyl)-*N*,*N*-di-(2-pyridylmethyl)amine; BMPA-Pr = *N*-propanoate-*N*,*N*-bis-(2-pyridylmethyl)amine; N3Py^{2Ph}SEtCN = 3-((2-((((5-phenylpyridin-2-yl)(6-phenylpyridin-2-yl)methyl)(pyridin-2-ylmethyl)amino)methyl)phenyl)thio)propanenitrile; TMPzA = tris(3,5-dimethylpyrazol-1-ylmethyl)amine; T1Et$_4$^{i}PrIP = tris(1-ethyl-4-isopropyl-imidazolyl)phosphine, BMPA = bis(methylpyridyl)amine; L$_{KP}$ = tris((1-methyl-4,5-diphenyl-1*H*-imidazol-2-yl)methyl)amine; 6-COOH-tpa = bis(2-pyridylmethyl)(6-carboxyl-2-pyridylmethyl)amine; S^{Me_2}N$_4$(tren) = 3-((2-(bis(2-aminoethyl)amino)ethyl)imino)-2-methylbutane-2-thiol; (OSiPh$_2$)$_2$O = 1,3-di(oxidanyl)-1,1,3,3-tetraphenyldisiloxane; and S$_2$SiMe$_2$ = dimethyldi(sulfanyl)silane.

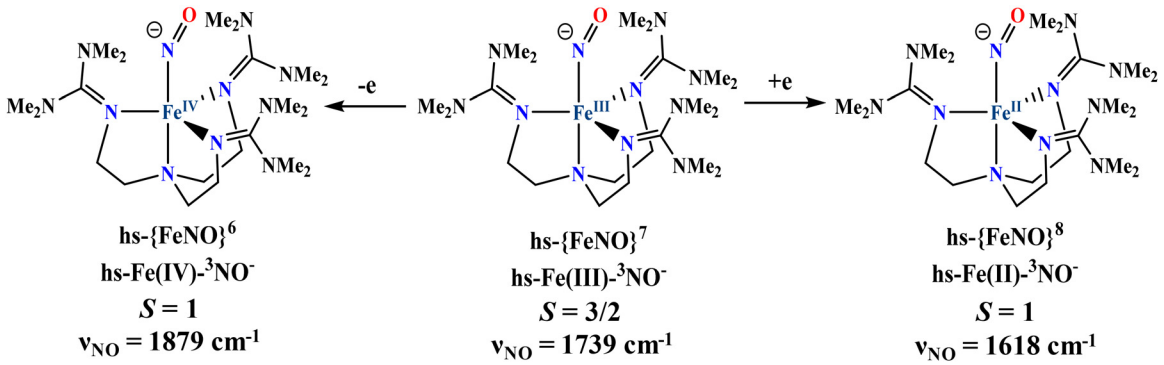

Fig. 2 Series of hs-{Fe–NO}$^{6-8}$ complexes using the TMG$_3$tren coligand reported by the Lehnert group,[26] where the redox transformations are all iron-centered.

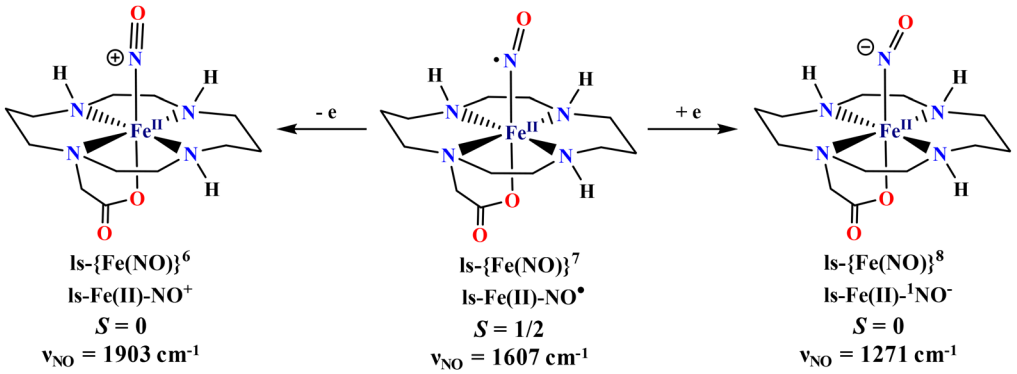

Fig. 3 Series of ls-{Fe–NO}$^{6-8}$ complexes using the cyclam-acetate coligand reported by the Wieghardt group,[31] where the redox transformations are all NO-centered.

and these complexes can be reduced to hs-{FeNO}^{8} complexes (S = 1, paramagnetic) at relatively mild redox potentials. The brown ring complex is also a hs-{Fe(NO)}^{7} species (S = 3/2), as confirmed by EPR and magnetic measurements (*vide infra*).

Prediction of the mode of coordination by the NO ligand in the brown ring complex

According to the Enemark–Feltham notation,[15] the 'Fe(NO)' moiety present in the brown ring complex is represented as {Fe(NO)}^{7}, where the superscript denotes the total number of valence electrons (*i.e.*, the sum of the metal-d and the NO-π* electrons) in the 'Fe(NO)' moiety. The value of total electron count (= 7) predicts a bent Fe–N–O linkage (*i.e.*, NO acting as a 1e donor ligand). This simple prediction is to be justified by the experimental findings and computational results. In fact, there is a difference of opinion in this regard among the different groups of workers, and it is still an active area of research for both computational chemists and experimental chemists.[36,46,50,61–66] The brown-ring complex was first proposed in 1958 by Griffith *et al.*[65] as an Fe(I) complex with NO^+, produced from Fe(II) through the reduction of Fe(II) by the odd-electron molecule NO, which is oxidised to closed-shell NO^+ to act as the ligand. Thus, all the seven electrons present in the 'Fe(NO)' moiety of the brown ring complex reside on the metal center Fe(I) (high-spin $t_{2g}^5e_g^2$, S = 3/2). The charge transfer transition within Fe(I) was considered to explain the broad absorption band at 450 nm.[66] This idea was changed by the group of van Eldik in 2002 from their kinetic and spectroscopic (electron paramagnetic resonance (EPR), Mössbauer (MB), IR and flash photolysis spectroscopy) studies (Fig. 4), and they proposed the brown ring complex as a complex of Fe(III) (high-spin $t_{2g}^3e_g^2$, S = 5/2) antiferromagnetically coupled to a triplet-NO^- ligand (S = 1) produced through the 1e-reduction of NO by Fe(II).[50] It makes the overall system a quartet (S = 3/2).

The isomer shift of the Mössbauer spectral data (zero-field ^{57}Fe MB data: isomer shift (δ) = 0.76 mm s^{-1}, ΔE_Q = 2.1 mm s^{-1}) strongly supports the presence of high-spin Fe(III) antiferromagnetically coupled to triplet $^3NO^-$ (S = 1), producing the observed spin quartet ground state (S = 3/2). In fact, the MB parameters of the brown ring complex are in good conformity with those of many non-heme high-spin {FeNO}^{7} systems, best described as the Fe(III)–NO^- complexes, where a high-spin Fe(III) center (S = 5/2) is coordinated to a triplet $^3NO^-$ ligand (S = 1), and the spins are antiferromagnetically coupled.[11,12,27,33,71]

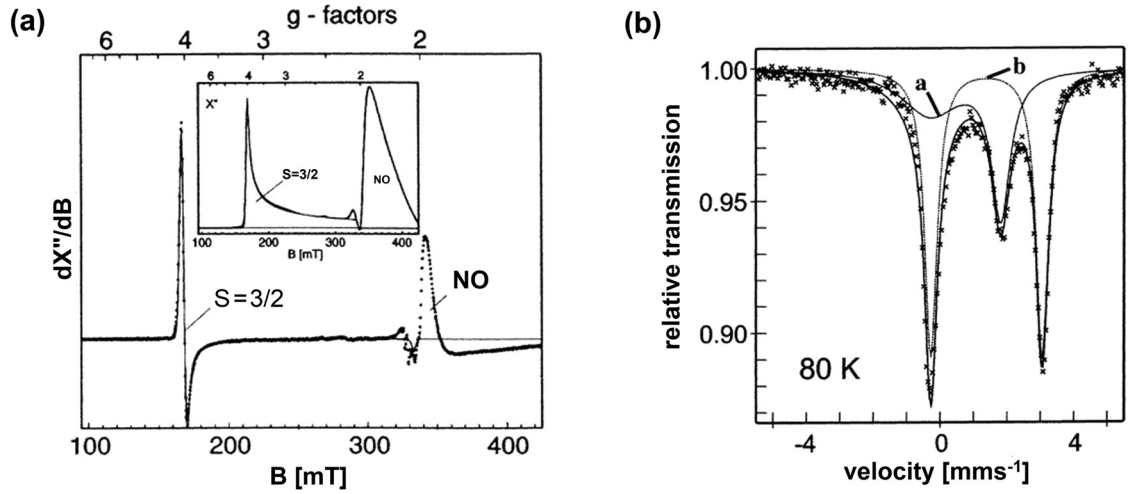

Fig. 4 (a) Experimental and simulated X-band EPR spectra of $[Fe(H_2O)_5(NO)]^{2+}$. The simulation shows effective g values g = 4.04, 4.04, and 2.0 [$D \gg h\nu$; E/D = 0] for a typical spin quartet species (trace 'S = 3/2'). (b) Zero-field Mössbauer spectrum of $[Fe(H_2O)_5(NO)]^{2+}$ at 80 K. Two overlapping quadrupole doublets with an intensity ratio of about 2 : 3. 'a' line for $\{FeNO\}^7$ (δ = 0.76 mm s^{-1}, ΔE_Q = 2.1 mm s^{-1}); 'b' line for unreacted $[Fe^{II}(H_2O)_6]^{2+}$. "Reprinted (adapted) with permission from ref. 50. Copyright {2002} American Chemical Society".

Recent studies further support this view. Goldberg *et al.*[48] recently reported one interesting example of a hs-$\{FeNO\}^7$ complex, $[Fe(N3Py^{2Ph}SEtCN)(NO)](BF_4)_2$, (see Table 2) generated from its hs-iron(II) precursor, $[Fe^{II}(CH_3CN)(N3Py^{2Ph}SEtCN)](BF_4)_2$. This hs-$\{FeNO\}^7$ complex (containing hs-Fe^{III}, antiferromagnetically coupled with the $^3NO^-$ ligand) exhibits δ = 0.67 mm s^{-1} and $|\Delta E_Q|$ = 2.20 mm s^{-1}, whereas the corresponding high spin Fe(II) precursor (S = 2) shows δ = 1.09 mm s^{-1} and $|\Delta E_Q|$ = 2.93 mm s^{-1}. The same group also reported another hs-$\{FeNO\}^7$ complex[55,58] (see Table 2), $[Fe(NO)(Me_3TACN)(OSiPh_2)_2O]$, with δ = 0.52 mm s^{-1} and $|\Delta E_Q|$ = 0.80 mm s^{-1}, again significantly lower than those of its high spin iron(II) precursor (δ = 0.98 mm s^{-1} and $|\Delta E_Q|$ = 1.98 mm s^{-1}). Similarly, Lehnert and co-workers[67] reported a non-heme high-spin $\{FeNO\}^7$ dimer, $[Fe_2(BPMP)(OPr)(NO)_2](OTf)_2$, described as Fe(III)–$^3NO^-$ with an isomer shift of δ = 0.70 mm s^{-1} and $|\Delta E_Q|$ = 1.72 mm s^{-1}, while its dinuclear Fe(II) precursor $[Fe_2(BPMP)(OPr)](OTf)_2$ exhibited an isomer shift of 1.19 mm s^{-1} and a quadrupole splitting $|\Delta E_Q|$ of 2.89 mm s^{-1}, which are both indicative of high-spin iron(II). Thus, the high-spin $\{FeNO\}^7$ complexes exhibit a much lower isomer shift (0.50–0.76 mm s^{-1}, see Table 2) than that of the corresponding high-spin iron(II) (S = 2) complexes.

Here, it may be noted that besides the oxidation state, some other factors, like the degree of covalency in the bond, may also partly contribute to determining the MB isomer shift.[27,63,68] In spite of this partial contribution of other factors, the MB isomer shift is considered as a strong evidence to identify the oxidation state of iron in its different compounds.[68–70] Thus, the observed MB isomer shift (0.76 mm s^{-1})[50] shows a convincing signature of hs-Fe(III) in the brown ring complex. Based on these observations, the former $[Fe^I(H_2O)_5(NO^+)]^{2+}$ complex was reformulated in 2002 as $[Fe^{III}(H_2O)_5(NO^-)]^{2+}$.[50]

Two years later, based on the computational studies (gas-phase DFT calculations), Cheng *et al.* proposed a new electronic structure for the complex as $[Fe^{II}(H_2O)_5(NO^0)]^{2+}$, *i.e.*, a complex of Fe(II) (high-spin $t_{2g}^4e_g^2$, S = 2), antiferromagnetically coupled to a doublet neutral NO ligand (S = 1/2).[61] Conradie *et al.* suggested the linearity of the Fe–N–O moiety in the ground state of the $\{Fe(NO)\}^7$ unit from their computational studies.[62] However, this prediction does not support the experimentally found bent structure of the Fe–N–O moiety in the brown ring complex.[46] These three possible electronic structures (a, b and c) are shown in Fig. 5.

All these structures explain the overall quartet state (S = 3/2) with the same magnetic moment (μ = 3.8 BM, suggesting three unpaired electrons) in conformity with the experimental findings.[65] Thus, the magnetic data measurements cannot discriminate among the three possible electronic structures. Because of the unstable nature of the brown ring complex, it was difficult to obtain the crystallographic data to characterise it. In this regard, Monsch *et al.* in 2019 made a major breakthrough by isolating the brown ring complex as the deep-brown crystals consisting mainly of $FeSO_4{\cdot}7H_2O$ = $[Fe(H_2O)_6](SO_4){\cdot}H_2O$ with small amounts (max. 14%) of the said nitrosyl complex bearing NO as a ligand replacing one water molecule.[46] Their crystal structure analysis using X-ray diffraction measurements (Fig. 6) indicated a bent Fe–N–O moiety (angle about 162°) in the crystalline environment.[46] They also analysed the bonding in the Fe–N–O moiety theoretically and concluded that because of the strong π-bonding interactions in the linkage, it is difficult to determine the oxidation state of iron in the brown ring complex.

The group of Odelius and Banerjee in 2022 suggested the dynamical instability of the brown ring complex that remains in an equilibrium mixture of octahedral $[Fe(H_2O)_5(NO)]^{2+}$ and square-pyramidal $[Fe(H_2O)_4(NO)]^{2+}$ species.[63] If there is an

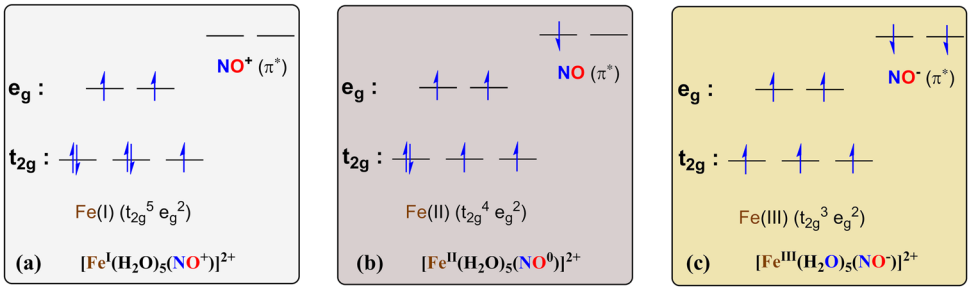

Fig. 5 Three possible electronic structures (a–c) of the brown ring complex $[Fe(H_2O)_5(NO)]^{2+}$ (S = 3/2).

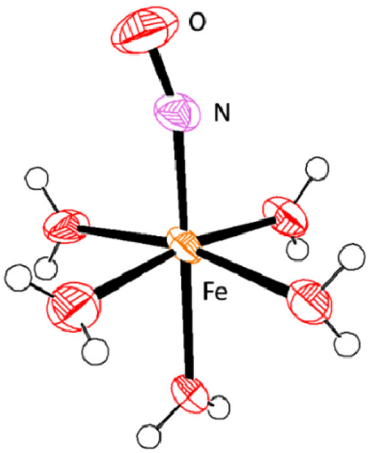

Fig. 6 The molecular structure of $[Fe(H_2O)_5(NO)]^{2+}$ in crystals of the ferrate, reported by the Klüfers group.[46] Bond distances: mean Fe–O_{aq} = 2.079 Å, Fe–N_{NO} = 1.780(3) Å, N–O = 1.134(4) Å; bond angles: Fe–N–O = 162.2(3)°; NO stretching frequency ν_{NO} = 1841 cm^{-1}; Mössbauer data: δ = 0.655(3) mm s^{-1} and $|\Delta E_Q|$ = 2.031(8) mm s^{-1}. Adapted from CCDC number 1893482.

equilibrium between these two species, obviously, the octahedral species is expected to be the predominant one because of the higher crystal field stabilisation energy (CFSE) in the octahedral geometry. The same group in 2023 proposed from theoretical calculations that the electronic structure of the 'FeNO' moiety in the brown ring complex depends on the Fe–N distance.[64] In 2025, a DMRG-CASSCF (DMRG-CASSCF denotes Density Matrix Renormalization Group – Complete Active Space Self-Consistent Field, CASSCF – a multireference method that accounts for these multiple configurations) study of $\{FeNO\}^7$ complexes by Ghosh *et al.* suggests that the brown ring complex ($[Fe(H_2O)_{4,5}(NO)]^{2+}$) predominantly exists as Fe(II) with neutral NO.[36]

To date, the structural interpretation of the brown ring complex has been made by the group of van Eldik[50] mainly through the experimental probes using different spectroscopic methods like IR, EPR, MB, and flash photolysis while the other groups have made most of the theoretical investigations using gas-phase calculations, implicit solvation models, *etc.*[36,61,63,64,73] If we consider the ligand environment in the brown ring complex having a large number of remaining σ-donor ligands ($5H_2O$), the low oxidation state of iron, like +1 state, is quite unlikely (*i.e.*, the reduction of Fe(II) to Fe(I) by NO producing an NO^+ ligand). Rather, to accommodate these large number of σ-donor ligands ($5H_2O$), a higher oxidation state of iron, like +2 or +3 state, is preferred.[13,14] If we consider the oxidation of Fe(II) to Fe(III) by NO, producing the NO^- ligand, then the experimental observations of EPR and MB spectroscopy can be nicely explained.[46,50] In fact, the presence of a large number of σ-donor ligands in $[Co(NH_3)_5(NO)]^{2+}$ leads to the chemical state as $[Co^{III}(NH_3)_5(NO^-)]^{2+}$.[12–14] The observed IR stretching frequency of NO in the brown ring complex is about 1810 cm^{-1} (*cf.* 1876 cm^{-1} for free NO having one electron in the π-ABMO, 2300 cm^{-1} for free NO^+ having no electron in the π-ABMO, and 1500–1600 cm^{-1} for free NO^- having two electrons in the π-ABMO).[11–14,50] It is important to note that the strength of the bonding interaction between $^3NO^-$ and Fe(III) in hs-$\{FeNO\}^7$ can be modulated by different factors[73] and is highly sensitive to the surrounding ligand environment.[11,12] For the 6-coordinate hs-$\{FeNO\}^7$ complexes, the N–O stretching frequency varies from 1848 to 1680 cm^{-1},[11,12] accompanied by variations in the Fe–N–O bond angle from 180 to 144° (see Table 2), and it depends on the types of coligands attached to the iron center.[11,12] A higher N–O stretching frequency is correlated with a more linear Fe–N–O unit.[16] Generally, the presence of neutral coligands coordinated to the iron center in the hs-$\{FeNO\}^7$ system leads to the higher N–O stretching frequencies.[12,16,43,45–53] On the other hand, the presence of the anionic coligands in the hs-$\{FeNO\}^7$ system leads to the lowering of N–O stretching frequency.[27,49–51,55–59] In the brown ring complex, the neutral coligands (H_2O) render the Fe center relatively electron-deficient, and the observed higher N–O stretching frequency (1810 cm^{-1})[50] can be explained by the greater π-donation from the π*-orbitals of $^3NO^-$ to Fe (d-orbitals), which reduces electron density in the N–O antibonding π-orbitals and strengthens the N–O bond.[12] The brown ring complex having the neutral coligands ($5H_2O$) records the bond angle of about 162°.[46] A similar type of bond angle (165°) and stretching frequency (1812 cm^{-1}) are observed in Goldberg's hs-$\{Fe(NO)\}^7$ complex, $[Fe(N3Py^{2Ph}SEtCN)(NO)](BF_4)_2$, where the coligand is also a neutral ligand.[48] However, the presence of anionic coligands in ochahedral hs-$\{FeNO\}^7$ complexes [*e.g.* $[Fe(NO)(Me_3TACN)((OSiPh_2)_2O)]$ (1680 cm^{-1}),[55,58] $[Fe(Me_3TACN)$

$(N_3)_2(NO)]$ (1690 cm^{-1}),[56] [Fe(BMPA-Pr)(Cl)(NO)] (1726 cm^{-1}),[49] $[Fe(6\text{-}COO^{-}\text{-}tpa)(NO)]^{+}$ (1752 cm^{-1}),[54] and [Fe(EDTA)(NO)] (1780 cm^{-1})[27,50] increases the electron density at the iron center. This results in reduced π-donation from $^{3}NO^{-}$, greater electron occupancy in the NO π* orbitals, weaker N–O bonds, and consequently, lower N–O stretching frequencies.

Here, it is worth mentioning that sodium nitroprusside (SNP) $Na_2[Fe^{II}(CN)_5(NO^{+})]$ ($S = 0$)[69–72] is considered to consist of ls-Fe(II) bearing an NO^{+} ligand. The ls-Fe(II) centre (t_{2g}^{6}) possesses a high CFSE (crystal field stabilisation energy) in sodium nitroprusside. In SNP, other remaining ligands are the π-acid ligands (5 CN^{-}) that favour the reduction of Fe(III) to Fe(II) by NO, producing the NO^{+} ligand and the reverse possibility, *i.e.* oxidation of Fe(II) to Fe(III) by NO, producing the NO^{-} ligand, is strongly disfavoured.[13,14] In fact, the group of π-acid ligands favours the lower oxidation state of the metal centre to enhance the metal-to-ligand back donation of electrons.

Conclusions

A single electronic state of the brown ring complex is not yet accepted by all. In fact, the strong π-bonding interaction in the Fe–N–O linkage of the brown ring complex complicates to determine the oxidation state of iron in the complex.[63] However, the structure $[Fe^{I}(H_2O)_5(NO^{+})]^{2+}$ involving the +1 state of iron and NO^{+} ligand proposed by Griffith *et al.* first in 1958 appears quite unlikely because it cannot adequately interpret the experimental findings like MB spectral data, stretching frequency of the NO group and bond angle (about 162°, bent Fe–N–O linkage, experimentally determined; *cf.* the NO^{+} ligand strongly favours a linear Fe–N–O linkage). Besides these, the +1 state of iron can hardly accommodate the large number of σ-donor ligands ($5H_2O$). Both the structures $[Fe^{II}(H_2O)_5(NO^{0})]^{2+}$ and $[Fe^{III}(H_2O)_5(NO^{-})]^{2+}$ lead to the bent Fe–N–O linkage as experimentally found and both Fe(II) and Fe(III) can also comfortably accommodate the remaining σ-donor ligands ($5H_2O$), but the structure involving hs-Fe(III) and $^{3}NO^{-}$ can better explain the spectroscopic data (IR, EPR, Mössbauer (MB), and flash photolysis spectroscopy) explored by the van Eldik group.[50] However, if we consider the structure $[Fe^{I}(H_2O)_5(NO^{+})]^{2+}$, then the extremely strong $d(Fe^{I}) \rightarrow \pi^{*}(NO^{+})$ π-back donation may lead to the higher oxidation state of iron like +2 or +3 or an intermediate state between +2 and +3.[63,73] In this concept, the limiting situation of π-back donation leads to the structure $[Fe^{III}(H_2O)_5(NO^{-})]^{2+}$ as proposed by the van Eldik group. To explain the blue-shifted stretching frequency (about 1800 cm^{-1}, higher than that of free NO^{-}) in the brown ring complex, the $\pi^{*}(NO^{-}) \rightarrow d(Fe^{III})$ donation is considered to deplete the electron density in the π*-MO of NO^{-}. Thus, the real oxidation state of iron represents most probably an intermediate state between +2 and +3, but closer to +3, which can explain the experimental observations of the van Eldik group and accommodation of the remaining σ-donor neutral ligands ($5H_2O$). The intense observed colour of the brown ring complex can be argued due to a ligand to metal charge transfer (LMCT) transition, $\pi^{*}(NO^{-}) \rightarrow d(Fe^{III})$. In fact, the origin of the color of $\{FeNO\}^{7}$ complexes due to the LMCT (NO^{-} to Fe(III)) transition has been analyzed in a number of cases.[12,26,27,74]

Conflicts of interest

The authors declare no conflicts of interest regarding this article.

Data availability

No primary research results, software or code have been included, and no new data were generated or analysed as part of this review.

Acknowledgements

The authors are grateful to Visva-Bharati University, Santiniketan, India, for providing the facilities to prepare the work. The authors acknowledge the encouragement and assistance offered by Prof. A. L. Koner, Department of Chemistry, Indian Institute of Science Education and Research (IISER) Bhopal, Madhya Pradesh, India. DM acknowledges financial support from the Science and Engineering Research Board (SERB), Government of India, New Delhi (SRG/2023/000511).

References

1 W. Manchot, DemonstrationsversuchemitFerrostickoxyd-Verbindungen, *Ber. Dtsch. Chem. Ges.*, 1914, **47**, 1614–1616.
2 N. N. Greenwood and A. Earnshaw, in *Chemistry of Elements*, Elsevier, New Delhi, 2nd edn, Indian reprint, 1997, p. 447, ISBN: 81-8147-806-1.
3 A. K. Das and M. Das, in *Fundamental Concepts of Inorganic Chemistry*, CBS Publishers & Distributors, New Delhi, 1st edn, 3rd reprint, 2019, vol. 7, p. 1673. ISBN: 978-81-239-2354-3.
4 A. K. Das and M. Das, in *Fundamental Concepts of Inorganic Chemistry*, CBS Publishers & Distributors, New Delhi, 1st edn, 3rd reprint, 2019, vol. 6, pp. 1373–1374. ISBN: 978-81-239-2353-6.
5 A. K. Das, *Resonance*, 2020, **25**(6), 787–799.
6 C. K. Jørgensen, *Coord. Chem. Rev.*, 1966, **1**, 164–178.
7 A. K. Das, M. Das and A. Das, in *Fundamental Concepts of Inorganic Chemistry*, CBS Publishers and Distributors Pvt. Ltd, New Delhi, 2nd edn, 2024, vol. 4, pp. 59–61. ISBN: 978-93-5466-189-1.
8 L. E. Laverman, A. Wanat, J. Oszajca, G. Stochel, P. C. Ford and R. van Eldik, *J. Am. Chem. Soc.*, 2001, **123**, 285–293.
9 M. Wolak, A. Zahl, T. Schneppensieper, G. Stochel and R. van Eldik, *J. Am. Chem. Soc.*, 2001, **123**, 9780–9791.

10 W. Kaim and B. Schwederski, *Coord. Chem. Rev.*, 2010, **254**(13–14), 1580–1588.
11 T. C. Berto, A. Speelman, S. Zheng and N. Lehnert, *Coord. Chem. Rev.*, 2013, **257**, 244–259.
12 N. Lehnert, E. Kim, H. T. Dong, J. B. Harland, A. P. Hunt, E. C. Manickas, K. M. Oakley, J. Pham, G. C. Reed and V. S. Alfaro, *Chem. Rev.*, 2021, **121**(24), 14682–14905.
13 A. K. Das and M. Das, in *Fundamental Concepts of Inorganic Chemistry*, CBS Publishers & Distributors, New Delhi, 1st edn, 3rd reprint, 2019, vol. 6, pp. 1357–1367. ISBN: 978-81-239-2353-6.
14 A. K. Das, M. Das and A. Das, in *Fundamental Concepts of Inorganic Chemistry*, CBS Publishers and Distributors Pvt. Ltd, New Delhi, 3rd edn, 2021, vol. 3B, pp. 46–48. ISBN: 978-93-90709-12-0.
15 J. H. Enemark and R. D. Feltham, *Coord. Chem. Rev.*, 1974, **13**, 339–406.
16 J. Li, A. Banerjee, P. L. Pawlak, W. W. Brennessel and F. A. Chavez, *Inorg. Chem.*, 2014, **53**, 5414–5416.
17 P. T. Manoharan and W. C. Hamilton, *Inorg. Chem.*, 1963, **2**, 1043–1047.
18 G. Paliani, A. Poletti and A. Santucci, *J. Mol. Struct.*, 1971, **8**, 63–74.
19 F. J. Bottomley, *Chem. Soc., Dalton Trans.*, 1974, **15**, 1600–1605.
20 E. E. Mercer, W. A. McAllister and J. R. Durig, *Inorg. Chem.*, 1966, **5**, 1881–1886.
21 T. E. Westre, A. Di Cicco, A. Filipponi, C. R. Natoli, B. Hedman, E. I. Solomon and K. O. Hodgson, *J. Am. Chem. Soc.*, 1994, **116**, 6757–6768.
22 A. A. D'Arpino, T. R. Cundari, P. T. Wolczanski and S. N. MacMillan, *Organometallics*, 2023, **42**, 2747–2761.
23 A. L. Speelman and N. Lehnert, *Acc. Chem. Res.*, 2014, **47**(4), 1106–1116.
24 A. L. Speelman and N. Lehnert, *Angew. Chem., Int. Ed.*, 2013, **52**, 12283–12287.
25 A. L. Speelman, B. Zhang, C. Krebs and N. Lehnert, *Angew. Chem., Int. Ed.*, 2016, **55**, 6685–6688.
26 A. L. Speelman, C. J. White, B. Zhang, E. E. Alp, J. Zhao, M. Hu, C. Krebs, J. Penner-Hahn and N. Lehnert, *J. Am. Chem. Soc.*, 2018, **140**(36), 11341–11359.
27 C. A. Brown, M. A. Pavlosky, T. E. Westre, Y. Zhang, B. Hedman, K. O. Hodgson and E. I. Solomon, *J. Am. Chem. Soc.*, 1995, **117**, 715–732.
28 T. A. Jackson, E. Yikilmaz, A.-F. Miller and T. C. Brunold, *J. Am. Chem. Soc.*, 2003, **125**, 8348–8363.
29 G. Schenk, M. Y. Pau and E. I. Solomon, *J. Am. Chem. Soc.*, 2004, **126**(2), 505–515.
30 A. R. Diebold, C. D. Brown-Marshall, M. L. Neidig, J. M. Brownlee, G. R. Moran and E. I. Solomon, *J. Am. Chem. Soc.*, 2011, **133**(45), 18148–18160.
31 R. G. Serres, C. A. Grapperhaus, E. Bothe, E. Bill, T. Weyhermüller, F. Neese and K. Wieghardt, *J. Am. Chem. Soc.*, 2004, **126**, 5138–5153.
32 N. Lehnert, K. Fujisawa, S. Camarena, H. T. Dong and C. J. White, *ACS Catal.*, 2019, **9**, 10499–10518.
33 Y. Zhang, M. A. Pavlosky, C. A. Brown, T. E. Westre, B. Hedman, K. O. Hodgson and E. I. Solomon, *J. Am. Chem. Soc.*, 1992, **114**(23), 9189–9191.
34 J. J. Yan, M. A. Gonzales, P. K. Mascharak, B. Hedman, K. O. Hodgson and E. I. Solomon, *J. Am. Chem. Soc.*, 2017, **139**, 1215–1225.
35 Q. M. Phung, H. N. Nam and A. Ghosh, *Inorg. Chem.*, 2023, **62**, 20496–20505.
36 Q. M. Phung, H. N. Nam, V. Austen, T. Yanai and A. Ghosh, *Inorg. Chem.*, 2025, **64**, 1702–1710.
37 J. Laane and J. R. Ohlsen, *Prog. Inorg. Chem.*, 2007, **27**, 465–513.
38 J. J. Weiss, *Nature*, 1964, **202**, 83–84.
39 J. S. Olson, A. J. Mathews, R. J. Rohlfs, B. A. Springer, K. D. Egeberg, S. G. Sligar, J. Tame, J. P. Renaud and K. Nagai, *Nature*, 1988, **336**, 265–266.
40 A. K. Das, M. Das and A. Das, in *Biophysical, Bioorganic & Bioinorganic Chemistry*, Books & Allied (P) Ltd, Kolkata, 2nd edn, 2021, pp. 345–398. ISBN: 978-81-948455-2-2.
41 A. K. Das, M. Das and A. Das, in *Bioinorganic Chemistry*, Books & Allied, Kolkata, 2nd edn, 2020, pp. 175–224. ISBN: 978-81-946982-1-0.
42 D. E. Milligan and M. E. Jacox, *J. Chem. Phys.*, 1971, **55**, 3404–3418.
43 A. Banerjee, J. Li, A. L. Speelman, C. J. White, P. L. Pawlak, W. W. Brennessel, N. Lehnert and F. A. Chavez, *Eur. J. Inorg. Chem.*, 2018, **2018**, 4797–4804.
44 M. Ray, A. P. Golombek, M. P. Hendrich, G. P. A. Yap, L. M. LiableSands, A. L. Rheingold and A. S. Borovik, *Inorg. Chem.*, 1999, **38**, 3110.
45 C. J. White, M. O. Lengel, A. J. Bracken, J. W. Kampf, A. L. Speelman, E. E. Alp, M. Y. Hu, J. Zhao and N. Lehnert, *J. Am. Chem. Soc.*, 2022, **144**, 3804–3820.
46 G. Monsch and P. Klüfers, *Angew. Chem., Int. Ed.*, 2019, **58**, 8566–8571.
47 S. Karmakar, S. Patra, K. Pramanik, A. Adhikary, A. Dey and A. Majumdar, *Inorg. Chem.*, 2024, **63**, 8537–8555.
48 A. M. Confer, S. Sabuncu, M. A. Siegler, P. Moënne-Loccoz and D. P. Goldberg, *Inorg. Chem.*, 2019, **58**, 9576–9580.
49 T. C. Berto, M. B. Hoffman, Y. Murata, K. B. Landenberger, E. E. Alp, J. Zhao and N. Lehnert, *J. Am. Chem. Soc.*, 2011, **133**, 16714–16717.
50 A. Wanat, T. Schneppensieper, G. Stochel, R. van Eldik, E. Bill and K. Wieghardt, *Inorg. Chem.*, 2002, **41**, 4–10.
51 H. T. Dong, A. L. Speelman, C. E. Kozemchak, D. Sil, C. Krebs and N. Lehnert, *Angew. Chem., Int. Ed.*, 2019, **58**, 17695–17699.
52 Y.-M. Chiou and J. L. Que, *Inorg. Chem.*, 1995, **34**, 3270–3278.
53 C. R. Randall, Y. Zang, A. E. True, L. Que, J. M. Charnock, C. D. Garner, Y. Fujishima, C. J. Schofield and J. E. Baldwin, *Biochemistry*, 1993, **32**, 6664–6673.
54 S. Karmakar, S. Patra, R. Halder, S. Karmakar and A. Majumdar, *Inorg. Chem.*, 2024, **63**(49), 23202–23220.
55 C. Hauser, T. Glaser, E. Bill, T. Weyhermuller and K. Wieghardt, *J. Am. Chem. Soc.*, 2000, **122**, 4352–4365.

56 K. Pohl, K. Wieghardt, B. Nuber and J. Weiss, *Chem. Soc., Dalton Trans.*, 1987, 187–192.
57 G. Villar-Acevedo, E. Nam, S. Fitch, J. Benedict, J. Freudenthal, W. Kaminsky and J. A. Kovacs, *J. Am. Chem. Soc.*, 2011, **133**, 1419–1427.
58 A. Dey, J. B. Gordon, T. Albert, S. Sabuncu, M. A. Siegler, S. N. MacMillan, K. M. Lancaster, P. Monne-Loccoz and D. P. Goldberg, *Angew. Chem., Int. Ed.*, 2021, **60**, 21558–21564.
59 A. Dey, T. Albert, R. Y. Kong, S. N. MacMillan, P. Moënne-Loccoz, K. M. Lancaster and D. P. Goldberg, *Inorg. Chem.*, 2022, **61**, 14909–14917.
60 T. Hayashi, J. D. Caranto, H. Matsumura, D. M. Kurtz Jr. and P. Moënne-Loccoz, *J. Am. Chem. Soc.*, 2012, **134**, 6878–6884.
61 H. Y. Cheng, S. Chang and P. Y. Tsai, *J. Phys. Chem. A*, 2004, **108**, 358–361.
62 J. Conradie, K. H. Hopmann and A. Ghosh, *J. Phys. Chem. B*, 2010, **114**, 8517–8524.
63 A. Banerjee, M. R. Coates and M. Odelius, *Chem. – Eur. J.*, 2022, **28**, e202200923.
64 M. R. Coates, A. Banerjee and M. Odelius, *Inorg. Chem.*, 2023, **62**, 16854–16866.
65 W. P. Griffith, J. Lewis and G. Wilkinson, *J. Chem. Soc.*, 1958, 3993–3998.
66 K. Ogura and M. Watanabe, *J. Inorg. Nucl. Chem.*, 1981, **43**, 1239–1241.
67 C. J. White, A. L. Speelman, C. Kupper, S. Demeshko, F. Meyer, J. P. Shanahan, E. E. Alp, M. Hu, J. Zhao and N. Lehnert, *J. Am. Chem. Soc.*, 2018, **140**, 2562–2574.
68 P. Gütlich, E. Bill and A. X. Trautwein, in *Mössbauer Spectroscopy and Transition Metal Chemistry*, Springer, Verlag Berlin Heidelberg, 2011.
69 N. N. Grennwood and T. C. Gibb, *Mössbauer spectroscopy*, Chapman and Hall Ltd, London, 1971, ISBN: 0-412-10710-4.
70 A. G. Maddock, *Mössbauer Spectroscopy Principles and Applications*, Horwood Publishing Limited, 1997, ISBN: 1-898563-16-0.
71 A. K. Das and M. Das, in *Fundamental Concepts of Inorganic Chemistry*, CBS Publishers & Distributors, New Delhi, 1st edn, 3rd reprint, 2019, vol. 7, pp. 1970–1971. ISBN: 978-81-239-2354-3.
72 A. Sadoc, R. Broer and C. de Graf, *Chem. Phys. Lett.*, 2008, **454**, 196–200.
73 M. Radoń, E. Broclawik and K. Pierloot, *J. Phys. Chem. B*, 2010, **114**(3), 1518–1528.
74 H. T. Dong, S. Camarena, D. Sil, M. O. Lengel, J. Zhao, M. Y. Hu, E. E. Alp, C. Krebs and N. Lehnert, *J. Am. Chem. Soc.*, 2022, **144**(36), 16395–16409.